Chapter

Effect of Roughness Elements on the Evolution of Thermal Stratification in a Cryogenic Propellant Tank

S.B. Vishnu and Biju T. Kuzhiveli

Abstract

The cryogenic propulsion era started with the use of liquid rockets. These rocket engines use propellants in liquid form with reasonably high density, allowing reduced tank size with a high mass ratio. Cryogenic engines are designed for liquid fuels that have to be held in liquid form at cryogenic temperature and gas at normal temperatures. Since propellants are stored at their boiling temperature or subcooled condition, minimal heat infiltration itself causes thermal stratification and self-pressurization. Due to stratification, the state of propellant inside the tank varies, and it is essential to keep the propellant properties in a predefined state for restarting the cryogenic engine after the coast phase. The propellant's condition at the inlet of the propellant feed system or turbo pump must fall within a narrow range. If the inlet temperature is above the cavitation value, cavitation will likely to happen to result in the probable destruction of the flight vehicle. The present work aims to find an effective method to reduce the stratification phenomenon in a cryogenic storage tank. From previous studies, it is observed that the shape of the inner wall surface of the storage tank plays an essential role in the development of the stratified layer. A CFD model is established to predict the rate of self-pressurization in a liquid hydrogen container. The Volume of Fluid (VOF) method is used to predict the liquid–vapor interface movement, and the Lee phase change model is adopted for evaporation and condensation calculations. A detailed study has been conducted on a cylindrical storage tank with an iso grid and rib structure. The development of the stratified layer in the presence of iso grid and ribs are entirely different. The buoyancy-driven free convection flow over iso grid structure result in velocity and temperature profile that differs significantly from a smooth wall case. The thermal boundary layer was always more significant for iso grid type obstruction, and these obstructions induces streamline deflection and recirculation zones, which enhances heat transfer to bulk liquid. A larger self-pressurization rate is observed for tanks with an iso grid structure. The presence of ribs results in the reduction of upward buoyancy flow near the tank surface, whereas streamline deflection and recirculation zones were also perceptible. As the number of ribs increases, it nullifies the effect of the formation of recirculation zones. Finally, a maximum reduction of 32.89% in the self-pressurization rate is achieved with the incorporation of the rib structure in the tank wall.

Keywords: Thermal stratification, self-pressurization, liquid hydrogen, iso grid, cryogenic tank

1. Introduction

Stratification in cryogenic liquid storage systems is a complicated yet inexorable thermodynamic phenomenon involving a combination of heat and mass transfer. Owing to the very low boiling point, they are susceptible to heat ingress from the ambient. Cryogenic propellant tanks undergo typical operation sequences when preparing for launch, including tank filling, chilling, boil-off, level correction, tank pressure and hold until lift-off. The time duration between tank pressurization and lift-off is called ground parking period. During ground parking, the heat ingress is due to the large temperature gradient existing between the storage and atmospheric temperature. An overwhelming increase in heat ingress occurs due to aerodynamic heating (during flight) and space radiation, although not as significant as the former, during coast phase. The insulation provided to the propellant tanks is foam which is relatively less effective compared to vacuum or multi-layered insulation (MLI). This heat leakage raises the temperature of liquid adjacent to the walls inducing natural convection currents. The heated liquid starts flowing up due to buoyancy and accumulates at the liquid-vapor interface creating an axial temperature gradient called thermal stratification. The depth of this stratified layer increases with time.

Consequently, the tank pressure keeps increasing due to vaporization. This demands the proper design of venting devices and insulation system. Hence thermal stratification is a crucial design criterion for designing rocket fuel tanks. A schematic for thermal stratification is illustrated in **Figure 1**.

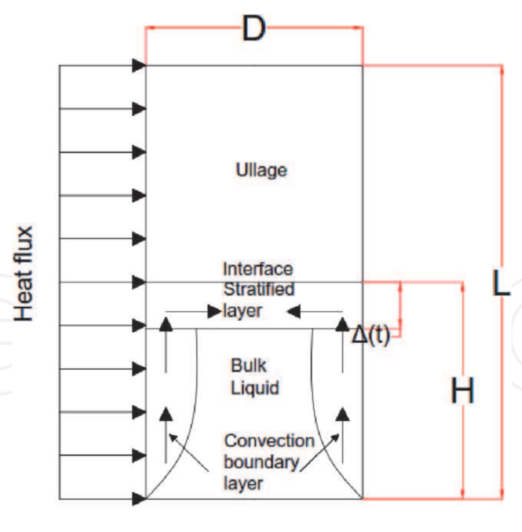

Figure 1.
Schematic of stratification phenomenon in a cylindrical tank.

2. Literature review

A wide variety of experimental and numerical studies have been conducted and reported by researchers across the globe on thermal stratification and self-pressurization of a cryogenic storage vessel. Tatom et al. [1] conducted an experimental investigation on a 500 - gal liquid hydrogen storage tank to provide stratification test data. The main objective of the study was to find out the effect of bottom heating on stratification. It was found that the controlled bottom heating can reduce the degree of stratification by transferring a large fraction of sidewall heat flux to bulk liquid. Schmidt et al. [2] conducted an experimental investigation to study pressurization and stratification of an LH2 tank and compared the results with the theoretical model. It is concluded that as interface temperature increases, the ullage pressure in the tank also increases, which results in more heat transfer to the stratified layer. The amount of additional heat transfer can be calculated using the theoretical model, which helps to optimize the pressure level within the storage tank. Ruder et al. [3] developed a mathematical method to determine the temperature profile inside a cryogenic storage tank under pressurized condition. They developed an empirical relation to represent the temperature profile which is similar in shape to a Gaussian probability distribution.

Several experimental kinds of researches on the evolution of thermal stratification and self-pressurization in a cryogenic storage tank have been reported in the literature. Aydelott et al. [4] developed a non-venting 9-inch diameter spherical container partially filled with liquid hydrogen for self-pressurization tests. The effects of filling per cent, heat flux, top heating, bottom and uniform heating were studied. It was found that the self-pressurization rate in the storage tank was mainly a function of the heating configuration with the per cent filling and heat-transfer rate playing a secondary role.

Ji et al. [5] conducted experiments on a heated container of liquid and developed various dimensionless parameters associated with thermal stratification. By comparing the dimensionless pressure and temperature, the quality of scaling was verified and concluded that parameters like tank pressure, bulk liquid temperature and the surface temperature could be scaled with dimensionless parameters. To study the self pressurization of a spherical liquid hydrogen tank, Hasan et al. [6] conducted an experimental investigation. The results showed that the initial conditions of the storage tank play a considerable role in self-pressurization. If the tank had previously experienced a steady boil-off rate due to long period venting, the self-pressurization rate seems to be lower and rapid pressurization rate was observed for the tank which is not at a steady venting condition. Yamaji et al. [7] conducted an experimental and numerical investigation of thermal stratification and plume mixing. Series of experiments were carried out using PIV and thermocouple measurements, and the developed CFX model reproduced the measured velocity distributions and temperature relatively well.

Gursu et al. [8] developed three different pressure rise models to predict thermal stratification and self-pressurization performance in cryogenic storage tanks; a homogeneous model, a surface evaporation model and a thermal stratification model. The thermal stratification model succeeds in predicting self-pressurization, whereas the other two models which are collectively the isothermal models could not predict the tank pressurization accurately enough. The flow pattern and thermal stratification of a cryogenic cylindrical tank were numerically studied by Chin-Shun Lin et al. [9]. The tank sidewall was subjected to either a uniform heat-flux or two discrete levels of uniform heat-flux at the upper and lower halves of the tank wall. The tank bottom was kept at a constant temperature controlled by the heat exchanger of a thermodynamic vent system. They successfully solved dimensionless steady-state conservation equations by a finite-difference method. Li et al. [10] developed a numerical model to study the thermodynamic effect of heat in-leak into a cryogenic tank and validated the model with experimentation. In the upper part of the liquid, a steady vortex-like region is developed as the heat inleak starts. A large temperature difference in the vertical direction was visible but little temperature difference in radial direction because the radial flow is predominant in that region. It was concluded that thermal stratification exists only in sub-cooled liquid and heat in-leak depends on the void fraction of fluid close to the tank wall. A calculation model is developed by Liu et al. [11] to predict self-pressurization and thermal stratification phenomenon of a liquid hydrogen storage tank. The effect of gravity level, fill level and temperature of the wall on the development of stratification were analyzed using the developed model. The effect of thermal aspect ratio on the self-pressurization is studied experimentally by Kang et al. [12]. A double wall vacuum insulated liquid nitrogen storage tank is developed for experimental investigation and the results were validated with the homogeneous model. Because of the thermal stratification, the experimental results slightly differ from that predicted by homogeneous model. The results indicate that the thermal stratification is highly correlated with the thermal aspect ratio.

The effect of rib shape and material thermal conductivity on the development of stratification was numerically studied by Fu et al. [13]. They considered cylindrical ribbed tank with 50% fill volume and rib shapes of rectangular and semi-circular. Tank pressurization rate was found to be lower for rib materials of low thermal conductivity. Semi-circular ribbed tank underwent lesser self-pressurization in comparison with the rectangular ribbed case for same rib cross-sectional area and locations.

Khurana et al. [14] carried out numerical investigations to minimize the thermal stratification in LH2 tanks. By providing transverse wall ribs on the inner surface of the cylindrical tank, they succeeded in achieving a 30% reduction in the stratification parameter. A delayed stratification, as well as lesser natural heat transfer coefficient, is observed for the tank with the ribbed inner surface than smooth wall tank. Polideri et al. [15] conducted an experimental investigation to study transient natural convection on a vertical ribbed wall. They reported a reduction in convective heat transfer coefficient below the initial rib and enhancement past the last one. A reduction in heat transfer performance was reported by Tanda et al. [16] for a case of natural convective air flow over a heated ribbed plate. To obtain the distribution of heat transfer coefficient, Schlieren optical technique was used to reproduce thermal field, and it was found that the induced flow creates thermally inactive regions just upstream and downstream of each protruding element.

Experimental and numerical studies were conducted by Shakerin et al. [17] to find out the flow behavior of air over a heated wall with single and repeated, two-dimensional, rectangular roughness elements. The flow visualization studies confirm the formation of nearly stagnant regions between the ribs and surface heat flux in these regions was very low. So the presence of wall ribs did not contribute to heat transfer enhancement. Zhongqi et al. [18] used Volume of Fluid (VOF) method to investigate the depressurization and thermal stratification behavior of a liquid nitrogen tank with different baffle structures under microgravity conditions. By optimizing the baffle setting, a reduction of up to 54% in pressurization rate was achieved, which is an eye-catching improvement for extended duration missions. Justin Oliveira et al. [19] investigated the effect of isogrid on thermal stratification inside propellant tanks. Studies showed that the boundary layer thickness on the wall in a forced free stream flow was distinctly thicker (150–700%) than the equivalent flat plate boundary layer thickness. Isogrids can either enhance or suppress stratification rate compared to smooth tanks depending upon roughness size and tank conditions. Experimental and numerical studies were carried out by Faure et al. [20] to assess the boundary layer behavior over the propellant tank with mass saving isogrid structures. They revealed that more than 200% thicker velocity boundary layer is developed over isogrid wall than a smooth wall. It leads to rapid self-pressurization and enhanced fluid mixing.

The presence of roughness elements has been found to reduce thermal stratification. The effect of spacing to height ratios of transverse ribs, protrusion length, the conductivity of ribs on heat transfer performance has been studied extensively, but for flat vertical and horizontal heated plates. Influence of ribs and grid structure on the reduction of stratification on a cryogenic cylindrical tank demand more detailed investigation.

3. Numerical modeling

A numerical model using Ansys Fluent is developed to study the stratification and self-pressurization phenomenon in a cryogenic storage tank. Smooth wall condition is considered and VOF (Volume of Fluid) transient method is used for the simulation. The governing equations are:

Conservation of mass:

$$\frac{\partial \rho}{\partial t} + \nabla.\left(\rho \vec{V}\right) = 0 \tag{1}$$

Conservation of momentum:

$$\frac{\partial (\rho \vec{V})}{\partial t} + \nabla.\left(\rho \vec{V}\vec{V}\right) = -\nabla P - \rho\beta\vec{g}(T - T_0) + \nabla.\left[\mu_{eff}\left(\nabla\vec{V} + \nabla\vec{V}^T\right)\right] + \vec{F} \tag{2}$$

Conservation of energy:

$$\frac{\partial (\rho C T)}{\partial t} + \nabla.\left(\vec{V}(\rho C T + P)\right) = \nabla.\left(K_{eff}\nabla T\right) + S_h \tag{3}$$

The location of the interface is identified by solving the continuity equation for the volume fraction of the second phase.

$$\frac{\partial}{\partial t}(\alpha_v \rho_v) + \nabla.\left(\alpha_v \rho_v \vec{V}\right) = \dot{m} \tag{4}$$

Where m represents the phase change mass at the interface due to evaporation or condensation. The density, viscosity and thermal conductivity is defined in terms of volume fractions.

$$\text{Density}, \rho = \alpha_l \rho_l + \alpha_v \rho_v \tag{5}$$

$$\text{Viscosity}, \mu = \alpha_l \mu_l + \alpha_v \mu_v \tag{6}$$

$$\text{Thermal conductivity}, k = \alpha_l k_l + \alpha_v k_{v.} \tag{7}$$

The assumptions used are,

1. The ullage pressure is determined by the saturation value corresponding to liquid–vapor interface.

2. The atmospheric temperature is considered as steady.

3. The ullage pressure is assumed to be uniform throughout.

Boundary conditions:
On the side walls,

$$-K\frac{\partial T}{\partial n} = q_w \tag{8}$$

At the bottom and top surfaces, the walls are adiabatic,

$$\frac{\partial T}{\partial n} = 0 \tag{9}$$

Where n is the direction normal to the wall

3.1 Numerical implementation

A cylindrical tank with 0.5 m diameter and 1 m height is used for the studies. The wall thickness is considered as 0.003 m and 2-D geometry is considered. Commercial CFD package Ansys 15 is used for solving the conservation equations. Axis-symmetric condition is selected because of the nature of physics, geometry and boundary conditions. The Rayleigh number corresponds to all operating condition is above the critical value and flow is always turbulent. So, k-ϵ turbulence model with enhanced wall function approach is applied. A constant heat flux of 10 W/m^2 is applied on the left sidewall. The pressure–velocity coupling algorithm selected is SIMPLEC (Semi-Implicit Method for Pressure-Linked Equation- Consistent). The converged solution is easy to achieve by using this method than a SIMPLE algorithm. The body forced weighted average scheme is used for solving the momentum equation. For tracking the liquid-vapor interface, the Geometric Reconstruction Scheme is applied. Since the problem is transient, a time step of 0.001 s is selected so that the Courant number is less than 0.1.

3.2 Grid independency

Three grid systems with mesh numbers 15288, 22893 and 30671 are used to test the resolution. **Table 1** shows the variation of pressure inside the tank with mesh number for the time period of 100 s. The self-pressurization for the two grids (22893 and 30671) is almost the same as the maximum pressure difference is less than 165 kPa. For the mesh number of 30671, the solution is time-consuming. The grids with 22893 quadrilateral grid elements are used with successively increasing mesh numbers towards the wall is selected for the present work.

Time (s)	Tank Pressure (Pa)		
	Grid no: 15288	Grid no: 22893	Grid no: 30671
10	101642	101690	101720
20	102057	102027	102030
30	102355	102392	102442
40	102610	102765	102838
50	102986	103134	103240
60	103214	103426	103555
70	103456	103640	103803
80	103614	103801	103929
90	103875	104060	104171
100	104012	104350	104483

Table 1.
Effect of mesh size on self-pressurization.

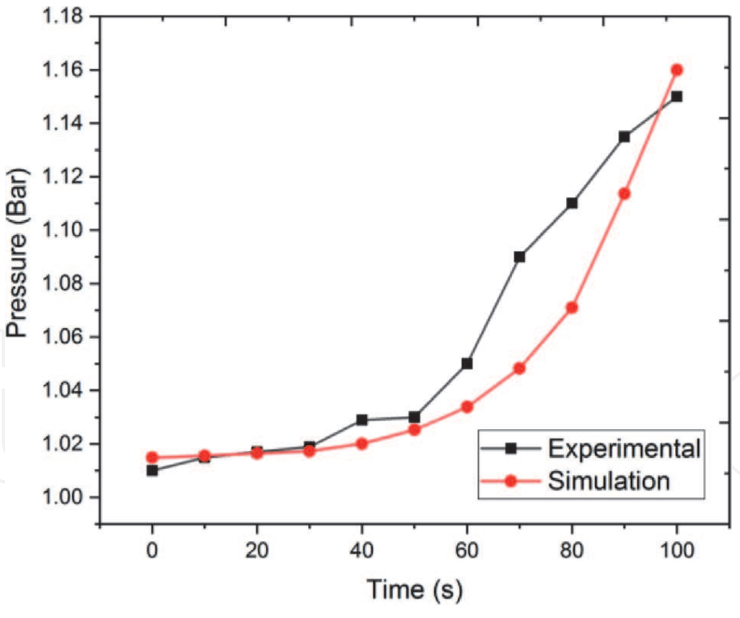

Figure 2.
Validation of the numerical model with experimental result.

3.3 Validation of the model

The numerical model developed has to be validated with the experimental results to prove the validity of the model in self-pressurization studies. The numerical model is validated with experiments conducted by Vishnu et al. [21]. The experiment set up consists of cylindrical test tank with a diameter of 0.11 m and height of 1.4 m. The liquid nitrogen cryogen was used as the model propellant and fill height was 0.7 m. The overall thermal conductivity of the tank wall was calculated as 0.01957 W/m.K for a tank thickness of 0.15378 m. Applying tank wall temperature of 300 K gives equivalent heat flux as that of experimental condition. The initial liquid temperature selected is 79.1 K which is equal to the initial interface temperature corresponds to the experimental condition and initial pressure corresponds to the saturation value of interface temperature. The initial temperature is assumed to be same throughout vapor and liquid domain. **Figure 2** compare the predicted pressure evolution against the experimental data. The maximum under-prediction of tank pressure by the numerical model compared to the experimental pressure data is not more than 2.6 percent. The tank numerical pressurization rate is in good agreement with the experiment, and hence self-pressurization is satisfactorily predicted.

4. Effect of obstruction elements

This section discusses about the impact of stratification due to the presence of roughness elements on the propellant tank wall. The nature of flow through a tank wall with roughness vary significantly to that of a smooth wall tank. The presence of roughness elements affects the formation of velocity and thermal boundary layer. The natural convection flow over a roughness element is more analogous to flow behavior over large scale obstruction elements such as forward-facing steps, backward facing steps, ribs and fences [20]. Based on the geometry, tank surface with obstruction elements can be classified as grids and ribs.

4.1 Comparison between flow over a smooth and rough wall

While comparing the performance of tanks with and without obstruction elements, proper scaling of tank geometry should be considered. Thermal stratification of a smooth wall with same liquid filling height as run length can be compared with that of a rough wall tank, but the volume of liquid and heated surface area will not be identical. Similarly, the heat flux applied could be matched but the filling height or run length would not be identical. In this analysis, the liquid filling height and tank radius considered are similar between smooth and rough wall tanks. Both tanks are having a radius of 0.25 m and filling height 0.5 m which is filled with liquid hydrogen. An axial heat flux of 10 W/m^2 is applied on the side wall. There are 25 number of obstruction elements with 0.178 cm height and 0.076 cm thickness. The details are shown in **Table 2**. The total run length along the obstruction surface is 108.9 cm which is 8.9% more than that of smooth wall tank. The smooth wall tank has a volume of 196349.54 cm^3 whereas rough wall tank has 196286.87 cm^3 which is 0.0319% lesser than smooth wall. The total heated surface area of rough wall tank is 17105.008 cm^2 which is 8.90% more than smooth wall tank and hence the volume to surface area ratio becomes 8.189% lesser for rough wall tank. The tank geometry and obstruction element layout is shown in **Figure 3**.

4.2 Comparison of flow through a smooth and rough surface tank

To study the effect of presence of obstruction elements on the natural convection flow, two cases were simulated. Flow through a smooth wall tank and flow through a storage tank with roughness elements at the inner wall surface. **Figure 4**

Parameter	Value
Tank height	1 m
Tank radius, R	0.25 m
Filling height, H	0.5 m
Grid height, h	0.178 cm
Grid thickness, t	0.076 cm

Table 2.
Geometrical parameters of tank.

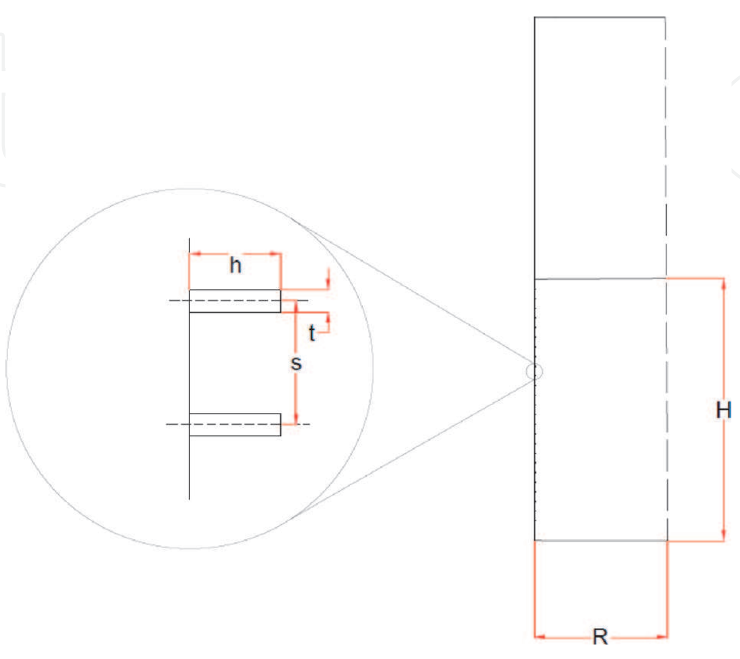

Figure 3.
Geometrical parameters of grids in a storage tank.

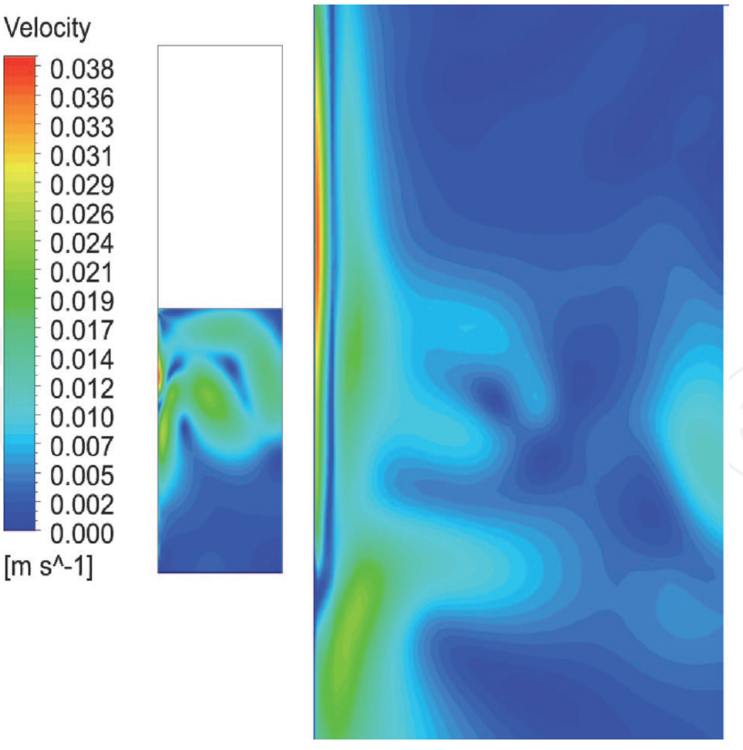

Figure 4.
Development of velocity boundary layer over a smooth surface tank.

shows the development of velocity boundary layer in a smooth tank wall due to natural convection flow. We can identify the development of laminar boundary layer and its magnitude keeps on increasing along the run length. The maximum velocity value of 0.038 m/s is obtained near to tank wall which is indicated as red color zone. Comparatively stagnant or undisturbed zones were developed at the bottom part of the bulk liquid zone.

Figure 5 shows the development of laminar boundary layer over a rough surface tank. Due to the presence of obstruction elements, we can see that the velocity near the tank wall is zero which is indicated by blue color zone. Also, stagnant regions are developed around the obstruction elements which causes further hindrance to the flow. Compared with smooth wall case, the bulk liquid seems undisturbed and flow due to natural convection takes place through the top face of the obstruction elements.

For the better understanding of the flow behavior over a tank surface with obstruction elements, stream line diagram can be used. The **Figure 6** shows the stream lines over a rough surface tank. It is clear that the flow gets obstructed with roughness elements. Stream line deflection also takes place due to the presence of obstruction elements. Apart from velocity distribution, the development of stratified layer greatly depends on the mechanism of heat transfer to the interface and bulk liquid.

Figure 7 shows the comparison of temperature contour over tank with smooth and roughness elements after 150 seconds of flow. The development of stratification and degree of stratification is higher for tank with obstruction elements. The presence of roughness elements causes the formation of stagnant regions near the wall but the increase in heat transfer area leads to better heat transfer to the fluid.

Figure 8 shows a detailed view of the development of thermal boundary layer over a tank with roughness elements. It can be seen that the boundary layer formed is almost uniform throughout the run length. It does not thicken monotonically along the wall. Due to increased surface area, there will be evident additional heating. So the temperature of liquid will be higher for rough wall case. The thermal

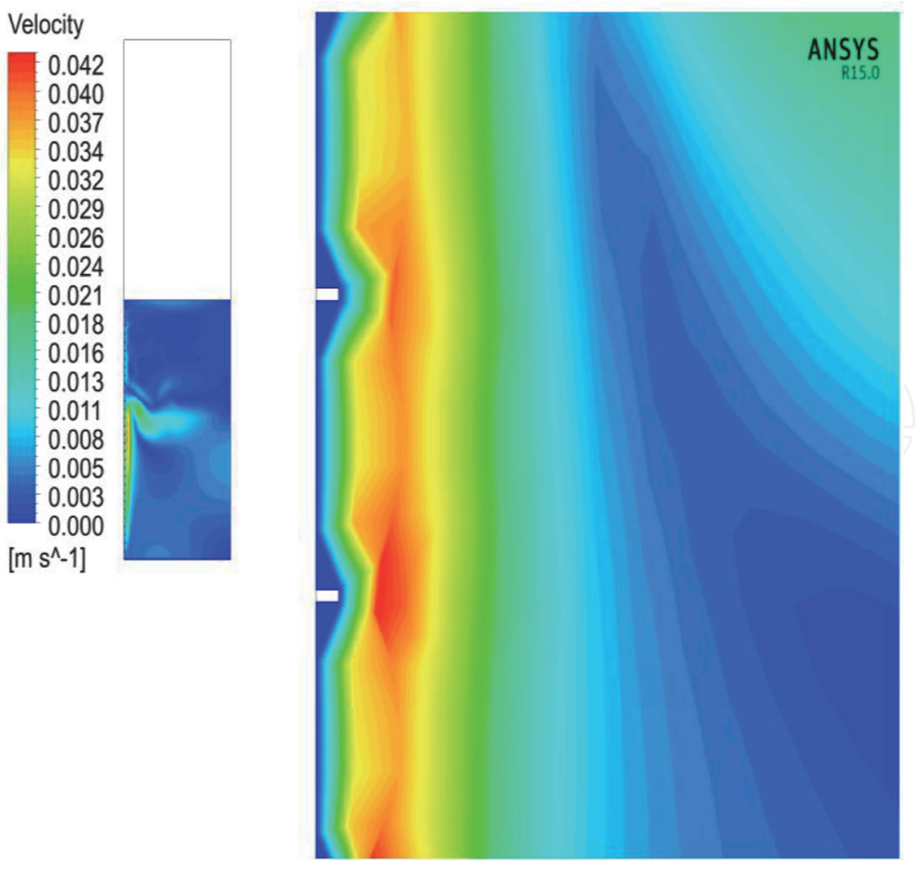

Figure 5.
Development of velocity boundary layer over a tank with obstruction elements.

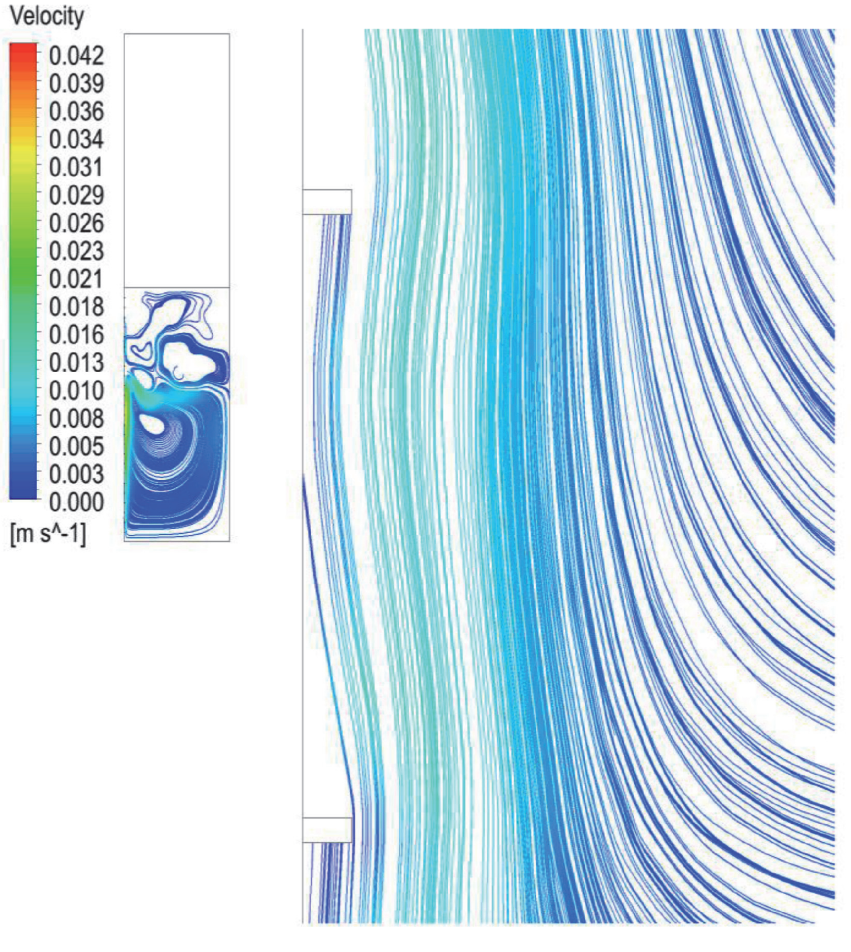

Figure 6.
Contour of stream lines over a tank with obstruction elements.

DOI: http://dx.doi.org/10.5772/intechopen.98404

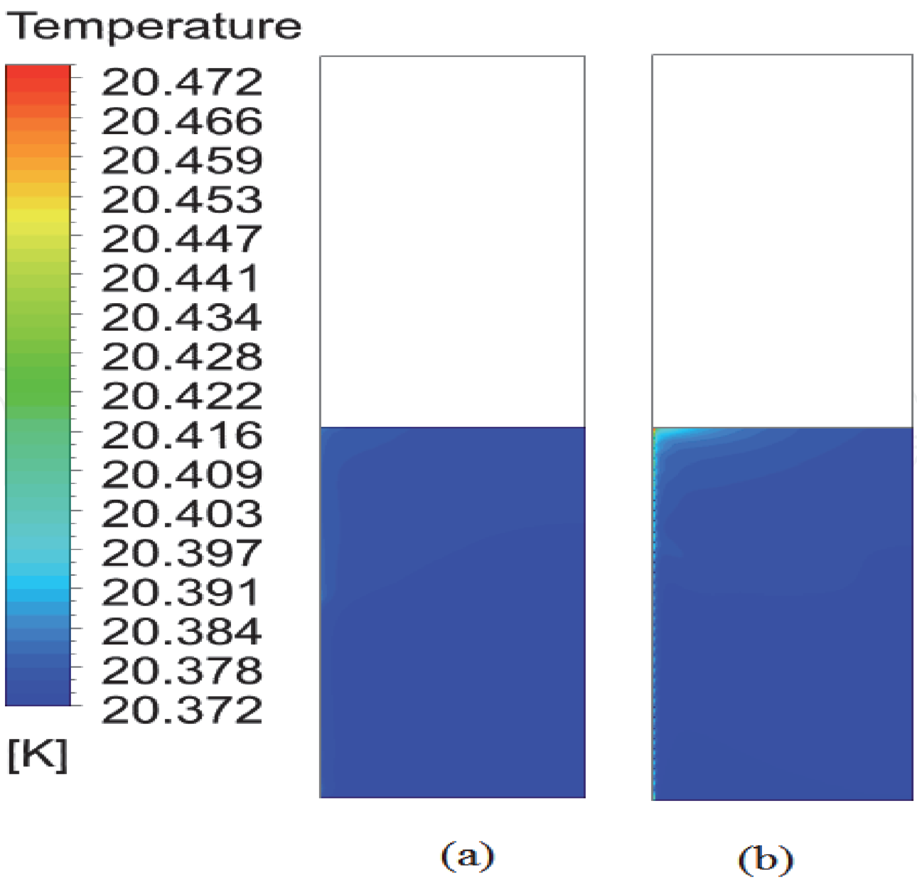

Figure 7.
Comparison of temperature contour over (a) smooth wall and (b) rough surface tank.

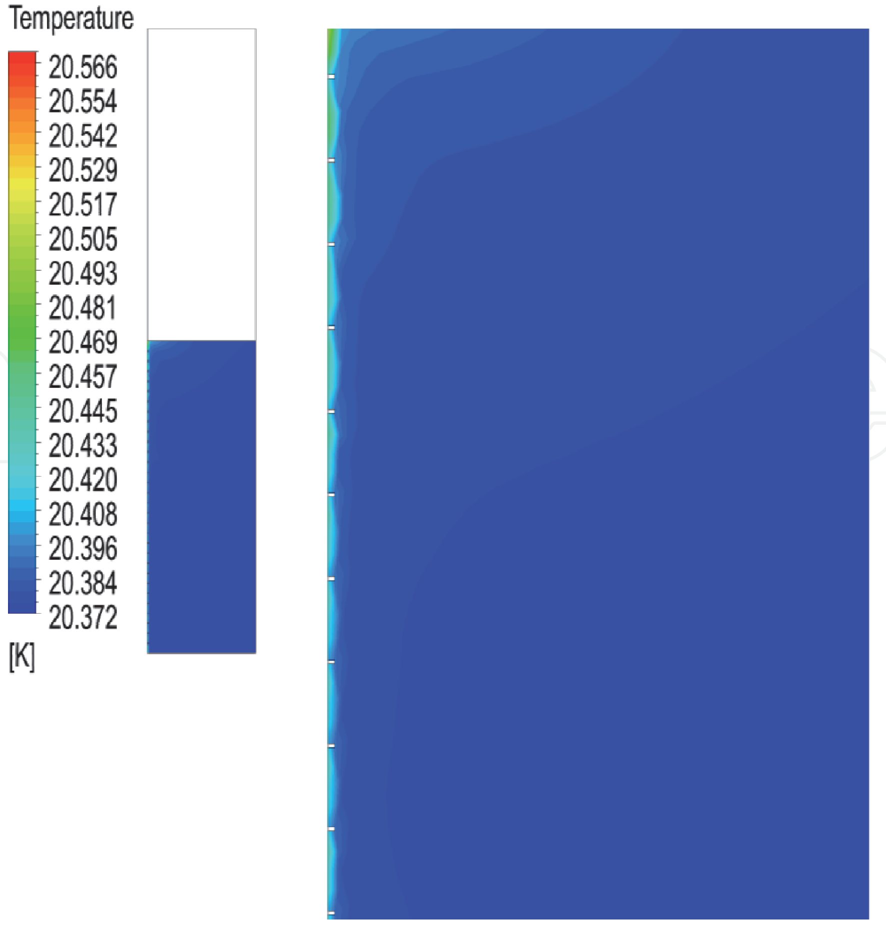

Figure 8.
Temperature contour of a liquid hydrogen tank with isogrids on the inner surface.

boundary layer developed is also thicker for rough wall case which further results in increased rate of thermal stratification and self-pressurization rate.

4.3 Thermal stratification in a cryogenic storage tank with isogrid surface

To study the impact on thermal stratification due to the presence of grids on tank wall, three cases were simulated. The roughness elements number varies such as 25, 30 and 35 corresponds to case 1, 2 and 3 respectively. For smooth wall case, the total volume of the tank is 196349.54 cm^3, the heated surface area is 15707 cm^2 and hence the volume to surface area ratio is 12.499. For tank with grids (case 1), the heated surface area increased to 17105.008 cm^2 and volume reduced to 196286.87 cm^2. So, the volume to surface area ratio reduces to 11.4754 which is 8.189%. Similarly, there is a reduction in volume to surface area ratio of 9.667% and 11.112% corresponds to case 2 and 3.

The evolution of pressure under three different cases is shown in **Figure 9**. As the number of elements increases, the value of pressure inside the tank also increases. The rise in pressure is noticeable after a time period of 60 seconds. It may due to the initial transient boundary layer formation process. As the number of roughness elements increases from 25 to 35, the heated surface area increases by 8.89% and 11.11%. It causes an increase in self-pressurization rate of 1.88 Pa/s (smooth wall) to 2.21 Pa/s (case 3). The case 3 with 35 number of obstruction elements have a self-pressurization rate which is 17.31% more than that of smooth wall case. The increase in self-pressurization rate due to presence of grids is shown in **Table 3**.

4.4 Thermal stratification in a cryogenic storage tank with rib surface

A similar kind of analysis is done incorporating ribs instead of grids on the tank wall. The rib geometry used in the analysis is having height ‘h’, spacing ‘s’ and

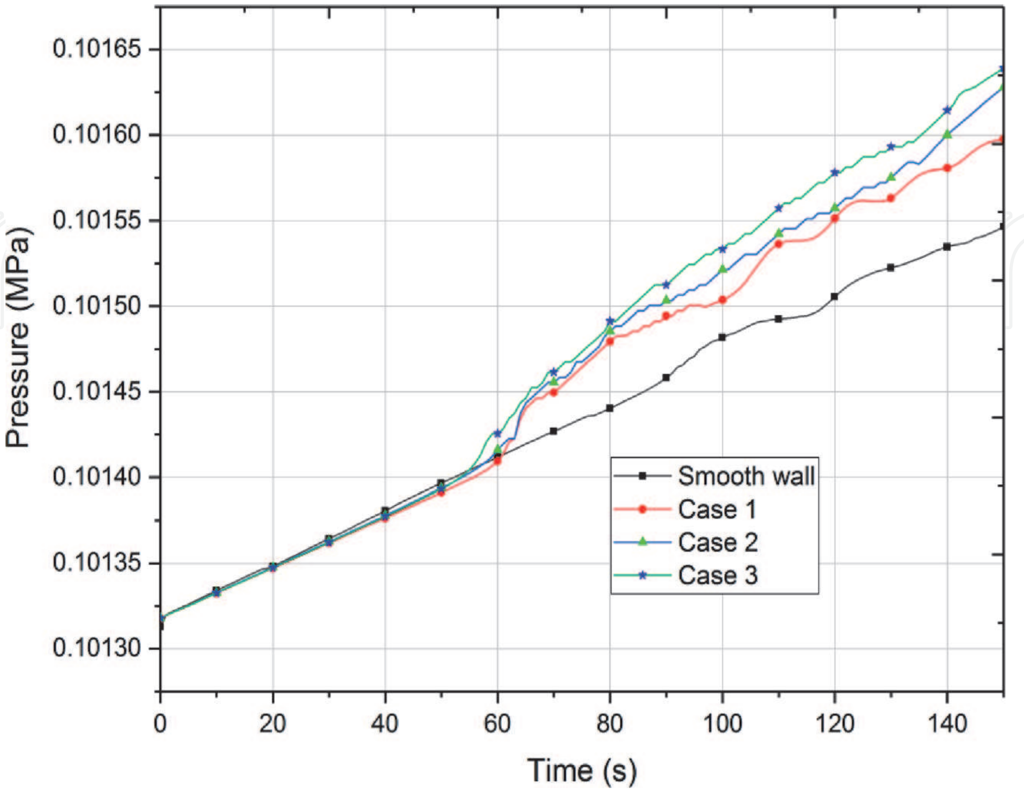

Figure 9.
Comparison of pressure evolution of a tank with different number of isogrids.

	Smooth wall tank	Case 1	Case2	Case3
Reduction in volume (%)	—	0.0319	0.0324	0.03787
Increase in heated surface area (%)	—	8.90	10.68	12.46
Reduction in VSA (%)	—	8.189	9.667	11.112
Increase in run length (%)		8.9	10.68	12.46
Self pressurization rate (Pa/s)	1.8866	1.92	2.1466	2.2133
Increase in SPR (%)	—	1.802	13.78	17.31

Table 3.
Influence of grid structure on the evolution of self-pressurization.

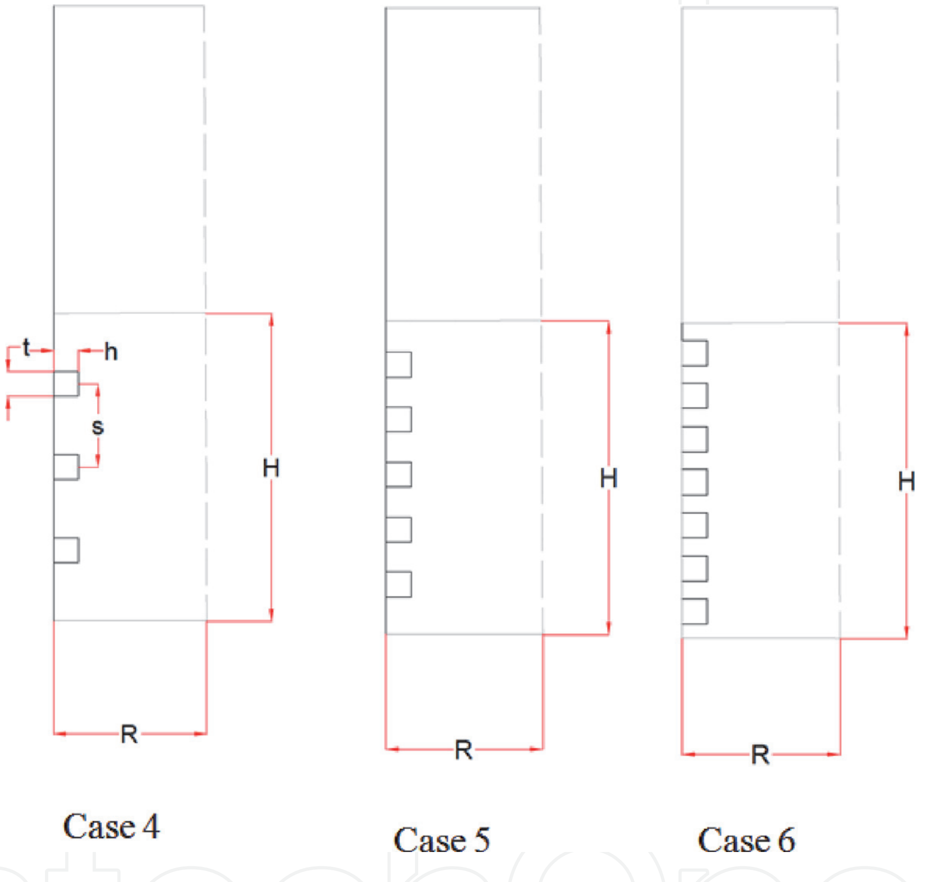

Figure 10.
Geometrical parameters of cylindrical tank with rib structure.

thickness 't' with rectangular cross section. The ribs were provided in the liquid side only. To study the effect of ribs on the evolution of stratification, three cases were considered; case 4, 5 and 6. Keeping the rib geometry and dimensions same, the distance between them is varied. So, the number of ribs corresponds to the cases 4 to 6 will be 3, 5 and 7 respectively. The tank geometry and rib layout are shown in **Figure 10**. The geometrical parameters are shown in **Table 4**.

Case	h (cm)	t (cm)	s (cm)
4	5	5	13.5
5	5	5	9
6	5	5	6.75

Table 4.
Geometrical parameters of ribs corresponds to cases 4–6.

For smooth wall case, the volume of the tank is 196349.54 cm^3 the heated surface area is 15707 cm^2 and hence the volume to surface area ratio is 12.499. For tank with 3 ribs (case 4), the volume reduces to 188809.7 cm^3 and heated surface area increases to 19476.91 cm^2. So, the volume to surface area ratio reduces to 9.694 which is 22.411%. Similarly, there is a reduction in volume to surface area ratio of 33.13% and 41.63% corresponds to case 5 and 6. Apart from these statistics, there is more increase in run length due to the presence of ribs. For case 4, the run length increases by 30%, 50% and 70% corresponds to case 5 and 6.

4.5 Effect of ribs on stratification

Figure 11 shows the velocity vector diagram for a tank with three grids (case 4). It is evident that the ribs create disturbance in the flow field, creating wake regions in the space between successive ribs. It affects the formation of boundary layer throughout the tank wall surface. Ultimately the presence of ribs enhances mixing in the bulk liquid which may reduce the formation of stratified layer.

The nature of flow velocities over three different configurations is depicted in **Figure 12**. The number of ribs affects the flow velocity inside the tank. Case 6 is having maximum number of ribs (7) which possess less velocity among the three cases. More number of ribs results in less flow velocity which indicates better mixing of bulk fluid and delayed stratification.

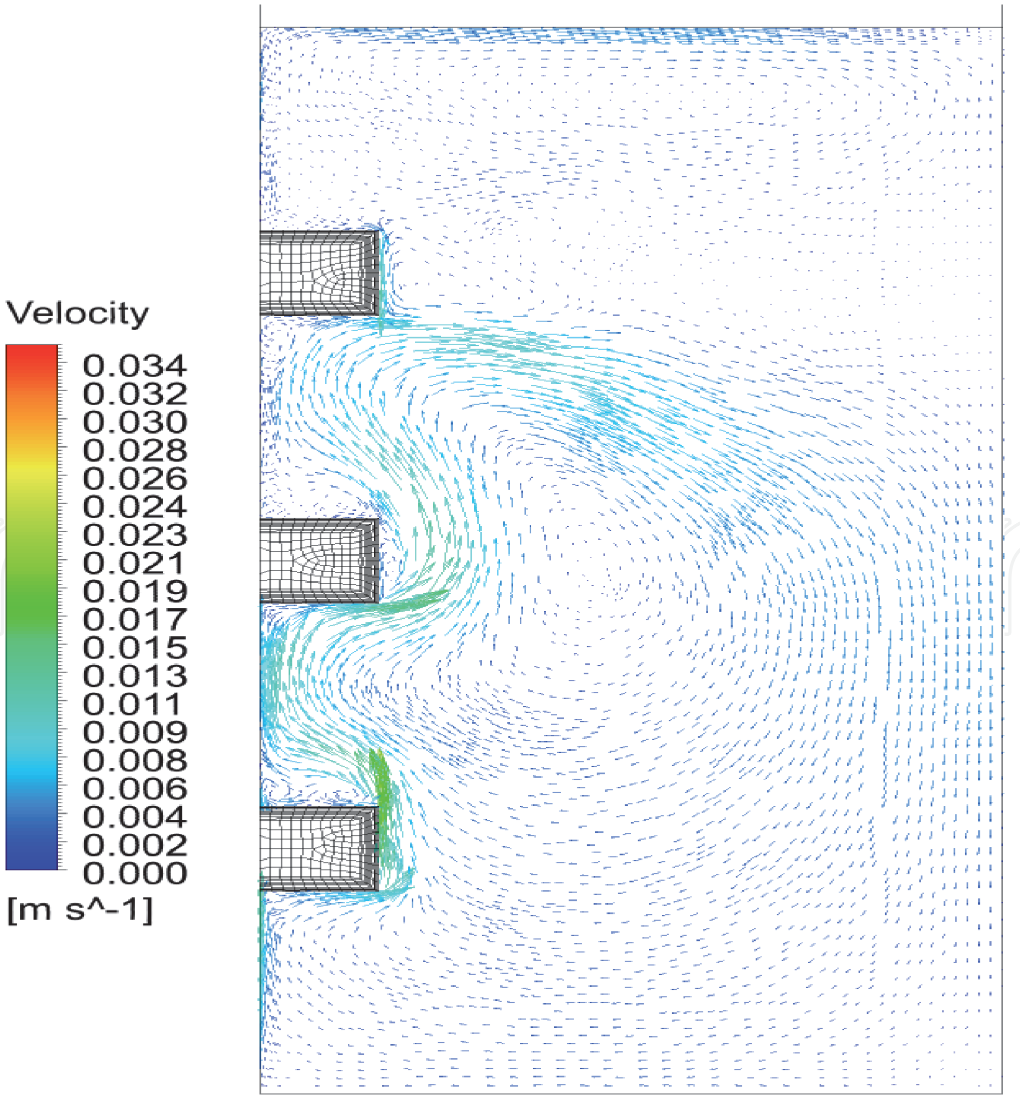

Figure 11.
Velocity vector diagram of a tank with rib structure.

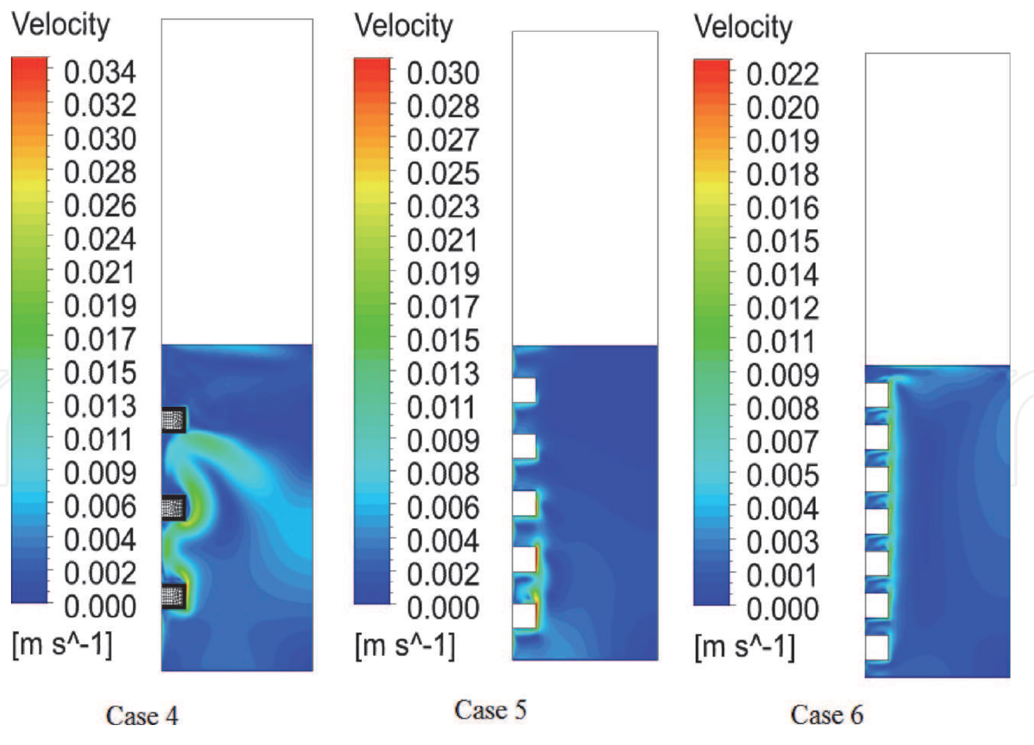

Figure 12.
Comparison of velocity of flow for cases 4–6.

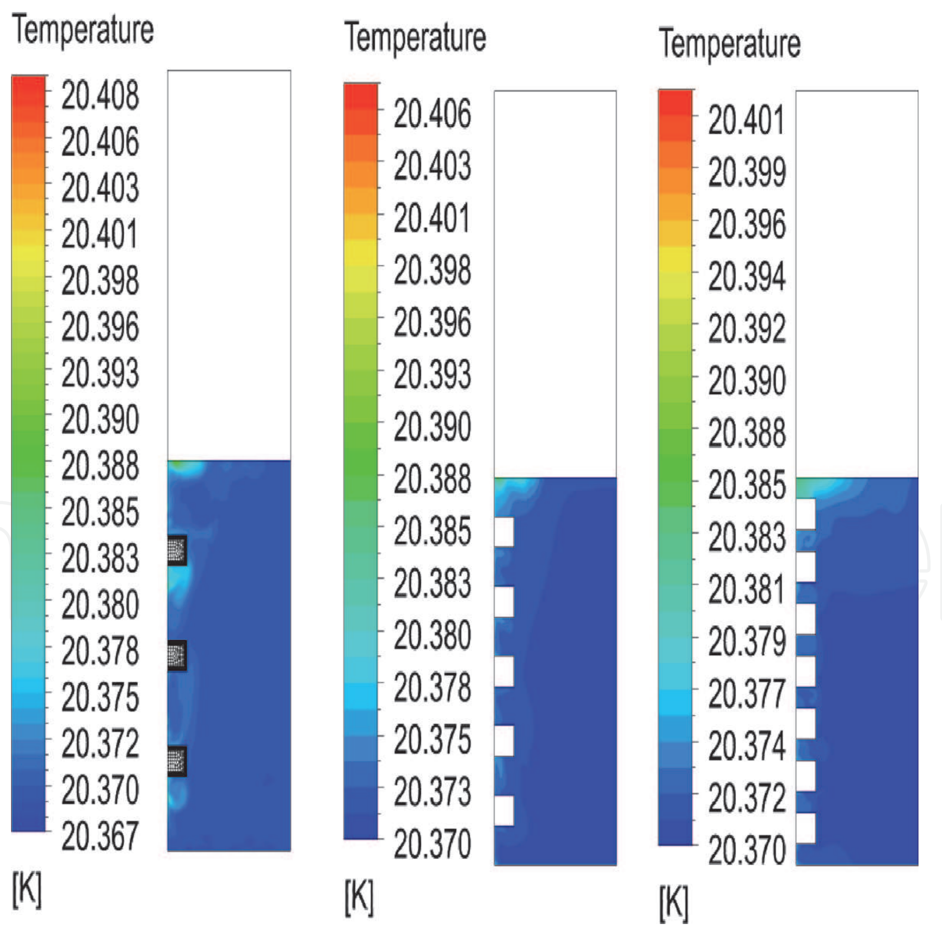

Figure 13.
Comparison of temperature of liquid for cases 4–6.

Figure 13 shows the comparison of temperature over three cases. Apart from interface, local heating zones were created on both sides of the rib surface. Since the presence of ribs causes obstruction of flow to a large extend, the locally heated fluid cannot travel to the interface effectively. The presence of recirculation zones enhances the mixing of the fluid. As a result, stratification develops very slowly. The formation of stratified layer is entirely different for three cases. There is more resembles between case 4 and smooth wall case. As the number of ribs increases, formation of local hotspots adjacent to the rib wall were visible and it is not transported to the interface. **Figure 14** shows the volume fraction under these cases.

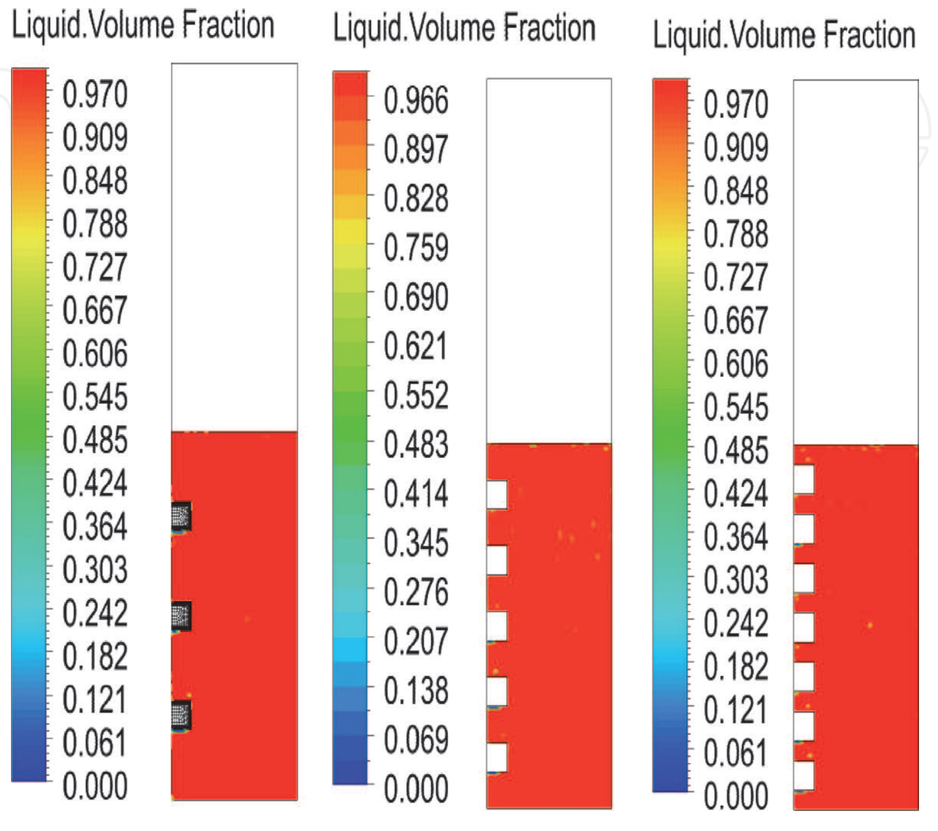

Figure 14.
Comparison of liquid volume fraction for cases 4–6.

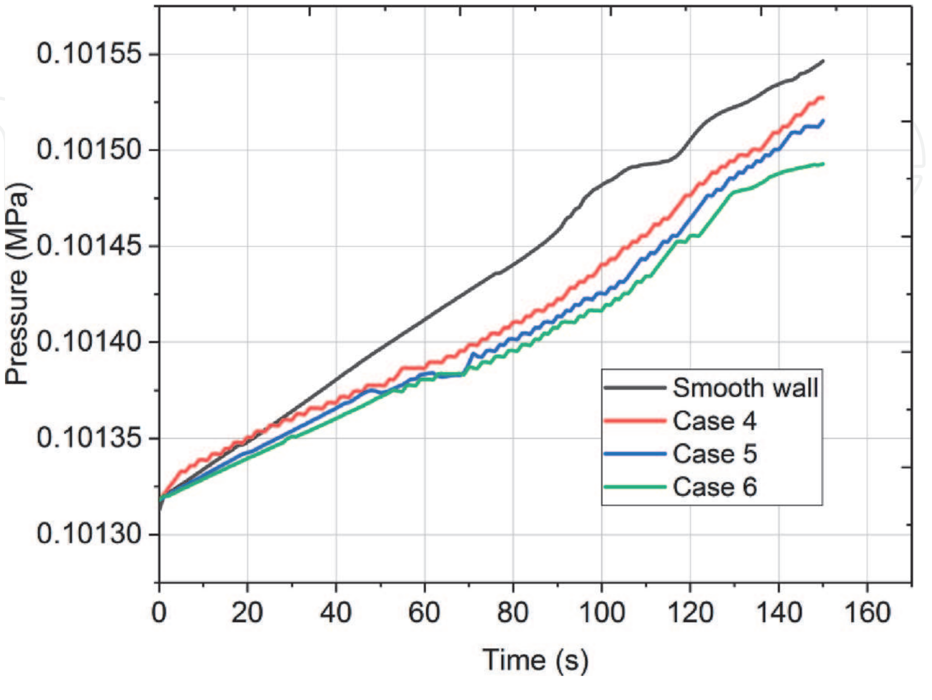

Figure 15.
Comparison of pressure evolution of a tank with different number of rib elements.

	Smooth wall tank	Case 4	Case5	Case6
Reduction in volume (%)	—	3.84	6.399	8.959
Increase in heated surface area (%)	—	24	40	56
Reduction in VSA (%)	—	22.441	33.13	41.63
Increase in run length (%)		30	50	70
Self pressurization rate (Pa/s)	1.8866	1.44	1.3533	1.266
Decrease in SPR (%)	—	23.67	28.26	32.89

Table 5.
Influence of rib structure on the evolution of self-pressurization.

Similar to temperature profile, the tank with more number of ribs has less phase change.

The evolution of pressure under three different cases is shown in **Figure 15**. As the number of ribs increases, the value of pressure inside the tank decreases and its value is well below that of smooth wall tank. The major change in pressure is noticeable after a time period of 70 seconds. As the number of grids increases from 3 to 7, the heated surface area increases by 24% and 56%. At the same time, a maximum reduction of 41.63% in volume to surface area ratio occurs for case 6. Ultimately the self-pressurization rate decreases by 32.89% for case 6. The decrease in self-pressurization rate due to presence of ribs is shown in **Table 5**.

5. Conclusions

A numerical model is developed to understand the effect of surface roughness elements on the evolution of stratification and self pressurization. The Volume of Fluid (VOF) method is used to predict the liquid–vapor interface movement, and the Lee phase change model is adopted for evaporation and condensation calculations. From previous studies, it is observed that the shape of the inner wall surface of the storage tank plays an essential role in the development of the stratified layer. Using the computational model developed, a detailed study has been conducted on a cylindrical storage tank with an iso grid and rib structure. The major conclusions are:

- The buoyancy-driven free convection flow over iso grid structure result in velocity and temperature profile that differs significantly from a smooth wall case.

- The thermal boundary layer was always more significant for iso grid type obstruction, and these obstructions induce streamline deflection and recirculation zones, which enhances heat transfer to bulk liquid.

- A larger self-pressurization rate is observed for tanks with an iso grid structure.

- The presence of ribs results in the reduction of upward buoyancy flow near the tank surface, whereas streamline deflection and recirculation zones were also perceptible.

- A maximum reduction of 32.89% in the self-pressurization rate is achieved with the incorporation of rib structure in the tank wall.

Nomenclature

C	Specific heat, J/kg.K
D	Diameter of the tank, m
F	Body force, N/m3
g	Acceleration due to gravity, m/s^2
H	Initial liquid height, m
K	Thermal conductivity, W/(m.K)
L	Total height of the vessel, m
$\dot{m}$	Mass flow rate, kg/s
P	Pressure, Pa
$\dot{q}$	Heat flux, W/m^2
S_h	Energy source term
T	Temperature, K
t	Time, s
$\vec{V}$	Velocity vector, m/s

Greek symbols

α	Volume fraction
μ	Absolute viscosity, Pa.s
ρ	Density, kg/m^3

Subscripts

h	Heat
l	Liquid
v	Vapor

Author details

S.B. Vishnu* and Biju T. Kuzhiveli
Centre for Advanced Studies in Cryogenics, National Institute of Technology Calicut, Calicut, India

*Address all correspondence to: vishnusb90@gmail.com

References

[1] J. W. Tatom, W. H. Brown, L. H. Knight, and E. F. Coxe, "Analysis of Thermal Stratification of Liquid Hydrogen in Rocket Propellant Tanks," *Adv. Cryog. Eng.*, pp. 265–272, 1964, doi: 10.1007/978-1-4757-0525-6_31.

[2] A. F. Schmidt, J. R. Purcell, W. A. Wilson, and R. V Smith, "An Experimental Study Concerning the Pressurization and Stratification of Liquid Hydrogen 1, 2," *J. Res. Natl. Bur. Stand. Eng. Instrum.*, vol. 65, no. 2, pp. 81–87, 1961.

[3] J. M. Ruder, "Stratification in a pressurized container with sidewall heating," *AIAA J.*, vol. 2, no. 1, pp. 135–137, 1964, doi: 10.2514/3.2242.

[4] J. C. Aydelott, "Normal gravity self-pressurization of 9-inch- (23 CM) diameter spherical liquid hydrogen tankage.," 1967.

[5] H. Ji, J. Hochstein, and S. Schwartz, "Experimental Verification of Scaling Parameters for Thermal Stratification," *AIAA Aerosp. Sci. Meet.*, 1990.

[6] M. M. Hasan, C. S. Lin, N. T. Van Dresar, F. Park, and C. S. L. Hasan, Mohammad M, "Self-Pressurization of a Flightweight Liquid Hydrogen Storage Tank Subjected to Low Heat Flux," *ASME/AIChE Natl. Heat Transfe Conf. Minneapolis, Minnesota, July 28-31,1991*, no. September, 1991.

[7] A. A. Yamaji, Rita Szijártó, "STUDY OF THERMAL STRATIFICATION AND MIXING USING PIV Bogdán Yamaji, Rita Szijártó, Attila Aszódi Institute of Nuclear Techniques, Budapest University of Technology and Economics."

[8] T. N. Veziroglu and J. W. Sheffield, "Analysis and Optimization of Thermal Stratification and Self-Pressurization Effects in Liquid Hydrogen Storage Systems — Part 2 : Model Results and Conclusions," vol. 115, no. September 1993, pp. 7–10, 2013.

[9] M. M. H. Chin-Shun Lin, "Numerical Investigation of the Thermal Stratification in Cryogenic Tanks Subjected to Wall Heat Flux," pp. 1–325, 2016, [Online]. Available: papers3://publication/uuid/40B251BA-DFAA-408F-AD41-E4BEBB70284E.

[10] X. Li, G. Xie, and R. Wang, "Experimental and numerical investigations of fluid flow and heat transfer in a cryogenic tank at loss of vacuum," *Heat Mass Transf. und Stoffuebertragung*, vol. 46, no. 4, pp. 395–404, 2010, doi: 10.1007/s00231-010-0583-9.

[11] Z. Liu, L. Wang, Y. Jin, and Y. Li, "Development of thermal stratification in a rotating cryogenic liquid hydrogen tank," *Int. J. Hydrogen Energy*, vol. 40, no. 43, pp. 15067–15077, 2015, doi: 10.1016/j.ijhydene.2015.09.039.

[12] M. Kang, J. Kim, H. You, and D. Chang, "Experimental investigation of thermal stratification in cryogenic tanks," *Exp. Therm. Fluid Sci.*, vol. 96, pp. 371–382, 2018, doi: 10.1016/j.expthermflusci.2017.12.017.

[13] J. Fu, B. Sunden, and X. Chen, "Influence of wall ribs on the thermal stratification and self-pressurization in a cryogenic liquid tank," *Appl. Therm. Eng.*, vol. 73, no. 2, pp. 1421–1431, 2014, doi: 10.1016/j.applthermaleng.2014.05.086.

[14] T. K. Khurana, B. V. S. S. S. Prasad, K. Ramamurthi, and S. S. Murthy, "Thermal stratification in ribbed liquid hydrogen storage tanks," *Int. J. Hydrogen Energy*, vol. 31, no. 15, pp. 2299–2309, 2006, doi: 10.1016/j.ijhydene.2006.02.032.

[15] G. Polidori and J. Padet, "Transient free convection flow on a vertical surface with an array of large-scale

roughness elements," *Exp. Therm. Fluid Sci.*, vol. 27, no. 3, pp. 251–260, 2003, doi: 10.1016/S0894-1777(02)00296-0.

[16] G. Tanda, "Natural convection heat transfer in vertical channels with and without transverse square ribs," *Int. J. Heat Mass Transf.*, vol. 40, no. 9, pp. 2173–2185, 1997, doi: 10.1016/S0017-9310(96)00246-3.

[17] A. Hadim and M. Ramot, "Natural convection in an enclosure with discrete heat sources on the vertical walls," *Am. Soc. Mech. Eng.*, vol. 31, no. 7, pp. 1–7, 1993.

[18] Z. Q. Zuo, W. B. Jiang, and Y. H. Huang, "Effect of baffles on pressurization and thermal stratification in cryogenic tanks under micro-gravity," *Cryogenics (Guildf).*, vol. 96, pp. 116–124, 2018, doi: 10.1016/j.cryogenics.2018.10.017.

[19] J. Oliveira, D. R. Kirk, S. Chintalapati, and P. A. Schallhorn, "Effect of isogrid roughness on thermal stratification," *Collect. Tech. Pap. - 43rd AIAA/ASME/SAE/ASEE Jt. Propuls. Conf.*, vol. 5, no. July, pp. 4734–4748, 2007, doi: 10.2514/6.2007-5497.

[20] J. M. Faure, J. M. Oliveira, S. Chintalapati, H. M. Gutierrez, and D. R. Kirk, "Effect of isogrid-type obstructions on thermal stratification in upper-stage rocket propellant tanks," *J. Spacecr. Rockets*, vol. 51, no. 5, pp. 1587–1602, 2014, doi: 10.2514/1.A32699.

[21] S. B. Vishnu, S. Bhowmick, and B. T. Kuzhiveli, "Experimental and Numerical Investigation of Stratification and Self pressurization in a High Pressure Liquid Nitrogen Storage Tank," *Energy Sources, Part A Recover. Util. Environ. Eff.*, vol. 0, no. 0, pp. 1–15, 2019, doi: 10.1080/15567036.2019.1651424.